

Stability and Hopf Bifurcation Analysis of a Phytoplankton-Zooplankton Model Under Temperature Factor and Stage-Structure Population of Phytoplankton

Nguyen Phuong Thuy*, Cao Thi Phuong, Van Duc An, Nguyen Duc Anh

Hanoi University of Science and Technology, Ha Noi, Vietnam

*Corresponding author email: thuy.nguyenphuong@hust.edu.vn

Abstract

In the paper, we built a predator-prey model to simulate and study the dynamics of zooplankton and phytoplankton populations under the temperature impact, in which the stage structure is considered in the zooplankton population. Our model is an ordinary differential system of three nonlinear equations with some parameters as temperature-dependent functions and uses the generalized Holling response function. The non-negative and boundedness of the model solutions have been proven. The behaviors of our system are shown by the local stability conditions of the equilibria, especially the co-existence case. The stage transformation of zooplankton was studied through the Hopf bifurcation results of varying the temperature. The analysis and simulation results indicate that the ideal temperature for the co-existence is about 12-21 degrees Celsius. The zooplankton's transformation decreases when the temperature increases, leading to an imbalance in the system. Besides that, we also provided simulation figures to illustrate the found theoretical results.

Keywords: Phytoplankton-zooplankton system, predator-prey model, stage-structure population, water temperature, stability analysis, Hopf bifurcation.

1. Introduction

In the aquatic environment, temperature is an essential factor affecting the growth of organisms. Aquatic organisms often seek out water areas with a suitable and stable temperature to live, reproduce and find food. Therefore, studying the effect of temperature on aquatic organism populations has attracted much attention in recent decades [1-4].

Plankton is tiny and temperature-sensitive organisms that live in water. We can divide them into three main groups: zooplankton, phytoplankton, and bacterioplankton. In particular, the interaction between zooplankton and phytoplankton plays an important role in balancing and maintaining nutrients in the aquatic ecosystem. Numerous studies have shown that ocean warming significantly impacts these two plankton organisms. For phytoplankton, Staehr and Sand-Jensen [5] investigated the effect of temperature on the rate of photosynthesis, respiration, and phytoplankton growth. Toseland *et al.* [6] studied these organisms' resource distribution and metabolism change when varying the temperature. For zooplankton, there were some relevant studies on the impact of temperature on the body-size decrease of Cladoceran species and the change in critical density with temperature [7]. Experimental results show that the change in water temperature can affect zooplankton's hunting ability and change the structure and the density of the phytoplankton population. From

that, the affection can lead to a significant variation in the marine food web.

Recently, Choi *et al.* [8] have proposed a mathematical model describing an ecosystem of three entities: nutrient source, phytoplankton, and zooplankton, in which phytoplankton contains toxin substances to run away from the zooplankton. In 2023, Gera [9] published the results about the effect of rainfall and temperature on plankton density in river flows. During the same period, a model to simulate the dynamics of a plankton population consisting of phytoplankton and their competition for nutrients was proposed by Chu *et al.* [10]. In 2021, there is also some typical research, like the results of Mandal *et al.* [11]. The authors studied the zooplankton and phytoplankton interaction, in which phytoplankton has a shelter and releases toxins to fight or counter the zooplankton. They pointed out that zooplankton can go extinct if the toxicity of phytoplankton is too high; meanwhile, providing more food sources will support the zooplankton's survival. Research is based on differential equations by Kulbhushan and Harpreet [12] on the possibility of optimal exploitation of phytoplankton in the case of zooplankton infected under the influence of toxicants. Their main results have shown that phytoplankton harvesting is vital in ecosystem dynamics while potentially controlling blooms. Sharada N.R *et al.* proposed a new model to study the stability of the zooplankton-phytoplankton

system, in which there are toxic phytoplankton and non-toxic phytoplankton [13]. Zooplankton tends to eat non-toxic phytoplankton, resulting in this phytoplankton can be eliminated soon and the toxic one thriving. Due to the lack of non-toxic prey, the competition in foraging by zooplankton is also increasing.

In this paper, we build a new mathematical model to study the interaction between zooplankton and phytoplankton under the effect of temperature and stage structure in the phytoplankton population. Our model is motivated by the proposed model in Zhao's research published in 2020 [14]. However, different from Zhao's model, our model uses the stage structure in the zooplankton population. In reality, the lifecycle of zooplankton has two main stages: larvae and adult, in which the temperature dramatically influences the transformation between them. The study by Jackson and Lenz discusses the increased predatory capability of zooplankton as they mature [15]. Larvae do not swim well, so they rely on ocean currents, while adults can use this ability to hunt. For simplicity, we consider larvae to be non-predatory. Moreover, larvae are less able to adapt to temperature than the adult stage, leading to a higher mortality rate. Some specific analyses regarding the temperature impact on the growth stages of zooplankton are presented in [16]. Therefore, the question that we want to answer is, for an ecosystem with the stage structure, how does temperature affect it? In our model, zooplankton consists of two stages: juvenile and adult, in which there exists a parameter representing the transform rate of zooplankton between these them. The equation for the dependence of density at two stages of zooplankton is shown separately.

The rest of this paper is organized as follows: In Section 2, we present our mathematical model and the ecological meaning of the parameters. The positivity, boundedness, and uniqueness of solutions, the stability analysis of the equilibrium points, and Hopf bifurcation results are analyzed and indicated in Section 3. Numerical simulations were performed to illustrate the theoretical results according to essential factors presented in Section 4. Finally, Section 5 gives some of our discussions and further work on this research.

2. The Mathematical Model

In this study, we investigate an ordinary differential system of three nonlinear equations as follows:

$$\begin{cases} \frac{dP}{dt} = r \left(1 - \frac{P}{K}\right) P - \frac{aP^n Z_A}{1+ahP^n}, \\ \frac{dZ_E}{dt} = -m_E Z_E - \alpha Z_E + e \frac{aP^n Z_A}{1+ahP^n}, \\ \frac{dZ_A}{dt} = \alpha Z_E - m_A Z_A. \end{cases} \quad (1)$$

The initial condition is considered as $P(0) > 0$, $Z_E(0) > 0$, $Z_A(0) > 0$. Parameter $n > 0$ is the Holling parameter of the response function. When $n = 1$, the response function is Holling type II, and when $n > 1$, we have the Holling type III response function. The variables P , Z_E and Z_A are the population density of phytoplankton, juvenile zooplankton, and adult zooplankton, respectively. The parameters r , K are the intrinsic growth rate and the maximum carrying capacity for phytoplankton. The parameter a is the capture rate of the adult zooplankton when foraging the phytoplankton and e is the transfer rate for reproduction from the phytoplankton found. The parameter h is the average time for processing food of zooplankton. Two parameters m_E , m_A are juvenile and adult zooplankton mortality rates, respectively. Finally, α is the transform rate of zooplankton from juvenile to adult.

To study the influence of temperature on the behavior of the multi-plankton dynamical system, we consider these above parameters as temperature-dependent functions [17] as follows:

1. The mortality rate: $m(T) = m_0 \exp\left(-\frac{E}{kT}\right)$.
2. The intrinsic growth rate of phytoplankton: $r(T) = r_0 \exp\left(-\frac{(T-T_{opt})^2}{(2S)^2}\right)$.
3. The capture rate: $a(T) = a_0 \exp\left(-\frac{(T-T_{opt})^2}{(2S)^2}\right)$.
4. The food processing time: $h(T) = h_0 \exp\left(\frac{(T-T_{opt})^2}{(2S)^2}\right)$.
5. The Holling parameter: $n(T) = n_0 \exp\left(\frac{(T-T_{opt})^2}{(2S)^2}\right)$.
6. The transform rate of zooplankton: $\alpha(T) = \alpha_0 \exp\left(-\frac{(T-T_{opt})^2}{(2S)^2}\right)$.

3. The Model Analysis

In this section, we derive the results of solutions' positivity, boundedness, and uniqueness to ensure the model consistent with reality. Besides that, the stability analysis of the equilibrium points and Hopf bifurcation are also presented.

3.1. The Positivity and Boundedness

Because the population densities are nonnegative and do not go to infinity, proof of the positivity and boundedness of the solution is necessary.

Theorem 3.1: All system (1) solutions are always positive and bounded.

Proof:

Firstly, we prove the positivity of solutions. Let $(P(t), Z_E(t), Z_A(t))$ be the solution of system (1) with the positive initial condition. We found that right-hand equations of (1) are continuous and smooth functions in $\mathbb{R}_+^3 = \{(P, Z_E, Z_A): P, Z_E, Z_A > 0\}$. For initial condition $P(0) > 0, Z_E(0) > 0, Z_A(0) > 0$, we have:

$$\begin{cases} P(t) = P(0)\exp\left(\int_0^t \left(r\left(1 - \frac{P}{K}\right) - \frac{aP^{n-1}Z_A}{1 + ahP^n}\right) ds\right) > 0, \\ Z_E(t) = Z_E(0)\exp\left(\int_0^t \left(-m - \alpha + e^{-\frac{aP^n Z_A}{(1 + ahP^n)Z_E}}\right) ds\right) > 0, \\ Z_A(t) = Z_A(0)\exp\left(\alpha\frac{Z_E}{Z_A} - m_A\right) > 0. \end{cases}$$

Therefore, all solutions of system (1) are always positive.

Next, we prove the boundedness. From the first equation of (1), we get:

$$\frac{dP}{dt} \leq r\left(1 - \frac{P}{K}\right)P.$$

Thus, we have:

$$\limsup_{t \rightarrow \infty} (P(t)) \leq K.$$

Let $\zeta(t) = eP(t) + Z_E(t) + Z_A(t)$ and replace to (1), we obtain:

$$\begin{aligned} \frac{d\zeta(t)}{dt} &= e\frac{dP}{dt} + \frac{dZ_E}{dt} + \frac{dZ_A}{dt} \\ &= er\left(1 - \frac{P}{K}\right)P - m_E Z_E - m_A Z_A \\ &\leq erP - (m_E Z_E + m_A Z_A) \\ &\leq 2erP - erP - (m_E Z_E + m_A Z_A) \\ &\leq 2erK - \min\{r, m_E, m_A\}(eP + Z_E + Z_A). \end{aligned}$$

We choose $\theta = \min\{r, m_E, m_A\}$, we have:

$$\frac{d\zeta(t)}{dt} + \theta\zeta(t) \leq 2erK.$$

Using differential inequality, we obtain:

$$0 \leq \zeta(t) \leq \frac{2erK}{\theta}.$$

Therefore, all solutions of (1) are bounded. Hence the theorem is proved.

3.2. The Uniqueness

The uniqueness is proven in the following theorem:

Theorem 3.2: For any initial value $(P(0), Z_E(0), Z_A(0)) \in \mathbb{R}_+^3$, the system (1) has a unique solution.

Proof:

Let $u(t) = \ln(P(t))$, $v(t) = \ln(Z_E(t))$ and $z(t) = \ln(Z_A(t))$, we have:

$$\begin{cases} \dot{u}(t) = r\left(1 - \frac{e^{u(t)}}{K}\right)e^{u(t)} - \frac{ae^{u(t)n}e^{z(t)}}{1 + ahe^{u(t)n}}, \\ \dot{v}(t) = -m_E e^{v(t)} - \alpha e^{z(t)} + e^{-\frac{ae^{u(t)n}e^{z(t)}}{1 + ahe^{u(t)n}}}, \\ \dot{z}(t) = \alpha e^{v(t)} - m_A e^{z(t)}. \end{cases} \quad (2)$$

where $t \geq 0$ and the initial value $u(0) = \ln(P(0))$, $v(0) = \ln(Z_E(0))$, $z(0) = \ln(Z_A(0))$.

Due to the coefficients of the system (2) satisfy the local Lipschitz condition, so system (2) has a unique solution $(u(t), v(t), z(t))$. Therefore, $(P(t), Z_E(t), Z_A(t)) = (e^{u(t)}, e^{v(t)}, e^{z(t)})$ is the unique solution of system (1) with the initial condition $(P(0), Z_E(0), Z_A(0)) \in \mathbb{R}_+^3$.

3.3. The Stability Analysis

Firstly, the system (1) has the following equilibrium point:

$$E_0 = (0, 0, 0).$$

$$E_1 = (K, 0, 0).$$

$$E^* = (P^*, Z_E^*, Z_A^*) \text{ where}$$

$$P^* = \left(\frac{m_A(m_E + \alpha)}{e\alpha\alpha - am_A h(m_E + \alpha)}\right)^{\frac{1}{n}},$$

$$Z_E^* = \frac{m_A}{\alpha} r \left(1 - \frac{P^*}{K}\right) \frac{1 + ahP^{*n}}{aP^{*(n-1)}},$$

$$Z_A^* = r \left(1 - \frac{P^*}{K}\right) \frac{1 + ahP^{*n}}{aP^{*(n-1)}}.$$

We have the Jacobian matrix of the system (1) as follows:

$$J = \begin{bmatrix} j_{11} & j_{12} & j_{13} \\ j_{21} & j_{22} & j_{23} \\ j_{31} & j_{32} & j_{33} \end{bmatrix} = \begin{bmatrix} r - \frac{2rP}{K} - \frac{anP^{n-1}Z_A}{(1 + ahP^n)^2} & 0 & -\frac{aP^n}{1 + ahP^n} \\ \frac{neaZ_AP^{n-1}}{(1 + ahP^n)^2} & -(m_E + \alpha) & \frac{eaP^n}{1 + ahP^n} \\ 0 & \alpha & -m_A \end{bmatrix}$$

Theorem 3.3 The equilibrium points E_0 is always unstable.

Proof:

For $E_0 = (0, 0, 0)$, we have the corresponding Jacobian matrix as follows:

$$J(E_0) = \begin{bmatrix} r & 0 & 0 \\ 0 & -(m_E + \alpha) & 0 \\ 0 & \alpha & -m_A \end{bmatrix}$$

We found that $J(E_0)$ has three eigenvalues with a positive one as follows:

$$\lambda_1 = r > 0;$$

$$\lambda_2 = -(m_E + \alpha) < 0;$$

$$\lambda_3 = -m_A < 0.$$

Thus, E_0 is unstable.

Theorem 3.4 The axial equilibrium points E_1 is stable if $m_A(m_E + \alpha) > \frac{aeaK^n}{1+ahK^n}$.

Proof:

We have the Jacobian matrix at E_1 as follows:

$$J(E_1) = \begin{bmatrix} -r & 0 & -\frac{aK^n}{1+ahK^n} \\ 0 & -(m_E + \alpha) & \frac{eaK^n}{1+ahK^n} \\ 0 & \alpha & -m_A \end{bmatrix}$$

The matrix $J(E_1)$ has three eigenvalues satisfy:

$$\begin{aligned} \lambda_1 &= -r < 0; \\ \lambda_2\lambda_3 &= m_A(m_E + \alpha) - \frac{aeaK^n}{1+ahK^n}; \\ \lambda_2 + \lambda_3 &= -(m_A + m_E + \alpha) < 0. \end{aligned}$$

Thus, if $m_A(m_E + \alpha) > \frac{aeaK^n}{1+ahK^n}$ then E_1 is stable. Hence, the theorem is proved.

Theorem 3.5: The equilibrium point E^* is locally asymptotically stable if and only if:

$$a_1 > 0, a_3 > 0 \text{ and } a_1a_2 > a_3,$$

where a_1, a_2, a_3 are the coefficients of λ in the characteristic equation at E^* as follows:

$$J(E^*) = \lambda^3 + a_1\lambda^2 + a_2\lambda + a_3.$$

Proof:

We have the Jacobian matrix at E^* as follows:

$$J(E^*) = \begin{bmatrix} j_{11} & 0 & j_{13} \\ j_{21} & -(m_E + \alpha) & j_{23} \\ 0 & \alpha & -m_A \end{bmatrix},$$

where $j_{11} = r - \frac{2rP^*}{K} - \frac{aP^{*(n-1)}Z_A^*}{(1+ahP^{*n})^2}$, $j_{13} = -\frac{aP^{*n}}{1+ahP^{*n}}$;

$$j_{21} = \frac{neaZ_A^*P^{*(n-1)}}{(1+ahP^{*n})^2}; j_{23} = \frac{eaP^{*n}}{1+ahP^{*n}}.$$

We have:

$$\det(J - \lambda I) = \begin{vmatrix} j_{11} - \lambda & 0 & j_{13} \\ j_{21} & j_{22} - \lambda & j_{23} \\ 0 & j_{32} & j_{33} - \lambda \end{vmatrix} \quad (3)$$

$$= \lambda^3 + a_1\lambda^2 + a_2\lambda + a_3,$$

where $a_1 = -j_{33} - j_{22} - j_{11}$,

$$a_2 = j_{11}j_{22} + j_{11}j_{33} + j_{22}j_{33} - j_{23}j_{32},$$

$$a_3 = j_{11}j_{23}j_{32} - j_{13}j_{21}j_{32} - j_{11}j_{22}j_{33}.$$

Using the Routh-Hurwitz criterion, E^* is asymptotically stable with the necessary and sufficient conditions as follows:

$$\begin{cases} a_1 > 0, \\ a_3 > 0, \\ a_1a_2 > a_3. \end{cases}$$

$$\Leftrightarrow \begin{cases} j_{33} + j_{22} + j_{11} < 0, \\ j_{12}j_{21}j_{32} + j_{11}j_{22}j_{33} - j_{11}j_{23}j_{32} < 0, \\ (j_{33} + j_{22} + j_{11})(j_{23}j_{32} - j_{11}j_{22} - j_{11}j_{33} - j_{22}) \\ > j_{11}j_{23}j_{32} - j_{13}j_{21}j_{32} - j_{11}j_{22}j_{33}. \end{cases}$$

3.4. Hopf Bifurcation

In this subsection, we investigate the stability of the co-existence equilibrium point when α is varied through the Hopf bifurcation. The characteristic equation at E^* is:

$$J(E^*) = \lambda^3 + a_1\lambda^2 + a_2\lambda + a_3, \quad (4)$$

where a_i with $i = 1, 2, 3$ is in Theorem 3.3.

Theorem 3.6: If exists $\alpha = \alpha^*$ satisfy:

$$\begin{aligned} i. & a_1a_2 = a_3, \\ ii. & \frac{a_1da_2}{d\alpha} + \frac{a_2da_1}{d\alpha} - \frac{da_3}{d\alpha} \neq 0, \end{aligned}$$

then, system (1) occurs Hopf bifurcation at the co-existence equilibrium E^* .

Proof:

We let the form of λ is $\lambda = u + iv$. Substituting λ into (3), we have:

$$\begin{aligned} (u + iv)^3 + a_1(u + iv)^2 + a_2(u + iv) + a_3 &= 0 \\ \Leftrightarrow u^3 + 3u^2vi - 3uv^2 - iv^3 + a_1u^2 - a_1v^2 & \\ + 2a_1uvi + a_2u + a_2vi + a_3 &= 0 \\ \Leftrightarrow u^3 - 3uv^2 + a_1u^2 - av^2 + a_2u + a_3 & \\ + (3u^2v - v^3 + 2a_1uv + a_2v)i &= 0. \end{aligned}$$

Thus, we get:

$$u^3 - 3uv^2 + a_1u^2 - a_1v^2 + a_2u + a_3 = 0; \quad (5)$$

$$3u^2v - v^3 + 2a_1uv + a_2v = 0. \quad (6)$$

From (6), representing v through u and substituting into (5), we have:

$$-8u^3 + 4a_1u^2 + u(2a_1^2 - 2a_2) - a_1a_2 + a_3 = 0.$$

Due to $u(\alpha^*) = 0$, differentiating (6) with respect to α and putting $\alpha = \alpha^*$, we obtain:

$$\left[\frac{du}{d\alpha} \right]_{\alpha=\alpha^*} = \left(\frac{\frac{a_1da_2}{d\alpha} + \frac{a_2da_1}{d\alpha} - \frac{da_3}{d\alpha}}{2a_1^2 - 2a_2} \right)_{\alpha=\alpha^*} \neq 0.$$

Thus, we get:

$$\frac{a_1da_2}{d\alpha} + \frac{a_2da_1}{d\alpha} - \frac{da_3}{d\alpha} \neq 0.$$

Hence, the theorem is proved.

4. Numerical Simulations

In this section, we provide the numerical simulations to illustrate the results in the above sections. Depending on the stability conditions in the above theorems, we can find the suitable temperature value with the parameter set so that the system (1) reaches the co-existence equilibrium point E^* .

For the parameter set chosen in Table 1, we compare the behavior of (1) with temperature values: $T = 14^\circ\text{C}$, $T = 20^\circ\text{C}$ and $T = 25^\circ\text{C}$. At $T = 14^\circ\text{C}$, the stable condition in Theorem 3.5 is not satisfied, so system (1) does not converge on E^* . Fig. 1 shows the behavior of the system (1) when $T = 14^\circ\text{C}$. In Fig. 1a, although we change the initial conditions, the system only converges on a limit cycle around E^* . Fig. 1b shows the time evolution of the density of three organisms, in which the values of the three density variables oscillate continuously over time with almost constant amplitude when the time is large enough. This shows that although the dynamical system does not have a stable equilibrium point, zooplankton and

phytoplankton can still co-exist in a relatively low-temperature environment.

On the contrary, when $T = 20^\circ\text{C}$, system (1) converges on the stable co-existence equilibrium point E^* . The time evolution of the system is shown in Fig. 2. Initializing with many different values (see Fig. 2a), the densities of organisms oscillate. However, the oscillation amplitude gradually decreases over time and finally converges to the equilibrium value when all two organisms co-exist (see Fig. 2b).

Fig. 3 shows the behavior of the system (1) when $T = 25^\circ\text{C}$. At this temperature value, the system converges on the free-zooplankton equilibrium E_1 where phytoplankton grows to the maximum carrying capacity K and the zooplankton is extinct. We can see that with the chosen parameter set, as the temperature increases, the behavior of the system is to change from the limit cycle to the co-existence equilibrium and to the free-zooplankton equilibrium point. Rising temperatures can be detrimental to zooplankton in the competition.

Table 1. Description of the parameters for model (1)

Parameter	Description	Values	Reference
m_E	Mortality rate of juvenile zooplankton	$m_{E0} = 20.8 \times 10^8$, $E = 0.55$, $k = 8.62 \times 10^{-5}$	-
m_A	Mortality rate of adult zooplankton	$m_{A0} = 20.4 \times 10^8$, $E = 0.55$, $k = 8.62 \times 10^{-5}$	-
α	Transform rate of zooplankton	$\alpha_0 = 0.8$, $S = 12$, $T_{opt} = 24$	-
r	Intrinsic growth rate of phytoplankton	$r_0 = 15$, $S = 12$, $T_{opt} = 25$	[15]
h	Food processing time	$h_0 = 0.17$, $S = 6.4$, $T_{opt} = 30$	[15]
a	Capture rate of zooplankton	$a_0 = 8.9$, $S = 9.4$, $T_{opt} = 22$	[15]
n	Holling parameter of functional response	$n_0 = 1.2$, $S = 22$, $T_{opt} = 16$	[15]
e	Conversion efficiency	0.274	-
K	Carrying capacity of environment	8	-

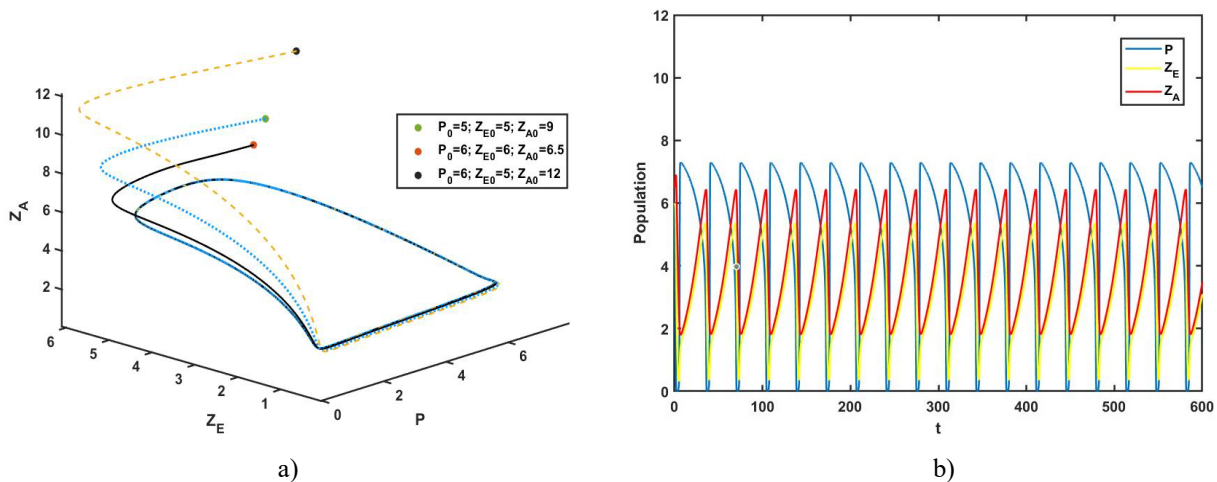


Fig. 1. Phase plot of model (1) a) and the behavior of plankton populations b) when $T = 14^\circ\text{C}$.

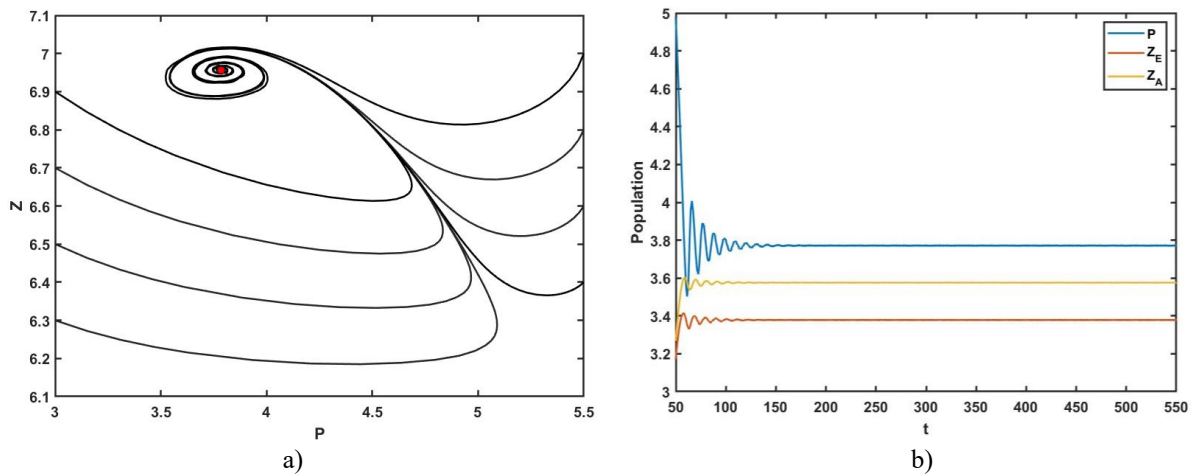


Fig. 2. Phase plot of model (1) a) and the behavior of plankton populations b) when $T = 20\text{ }^{\circ}\text{C}$.

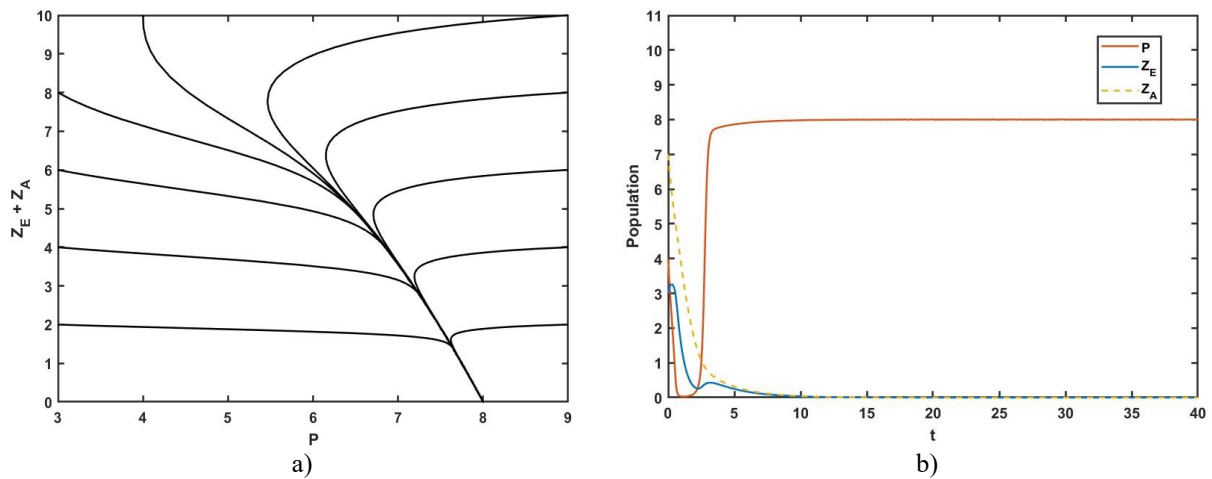


Fig. 3. Phase plot of model (1) a) and the behavior of plankton populations b) when $T = 25\text{ }^{\circ}\text{C}$.

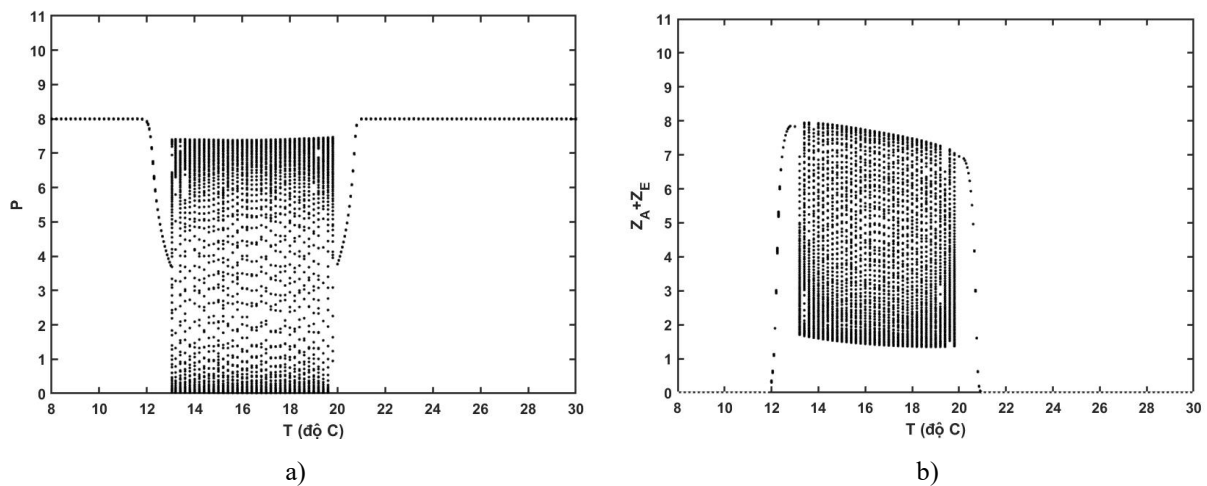


Fig. 4. Bifurcation diagrams respect to temperature of phytoplankton a) and zooplankton b) populations.

Fig. 4 shows more clearly the effect of temperature on the growth of two organism' populations. With the chosen parameter set, the best temperature range for the co-existence is about $12\text{ }^{\circ}\text{C} \sim 21\text{ }^{\circ}\text{C}$. However, in most of this temperature range, the two organism do not co-exist stably, their

densities oscillate continuously. Outside of this temperature range, zooplankton in both stages is eliminated. Only two temperature ranges $12\text{ }^{\circ}\text{C} \sim 13\text{ }^{\circ}\text{C}$ and $20\text{ }^{\circ}\text{C} \sim 21\text{ }^{\circ}\text{C}$, are ideal conditions for both organism populations to co-exist stably.

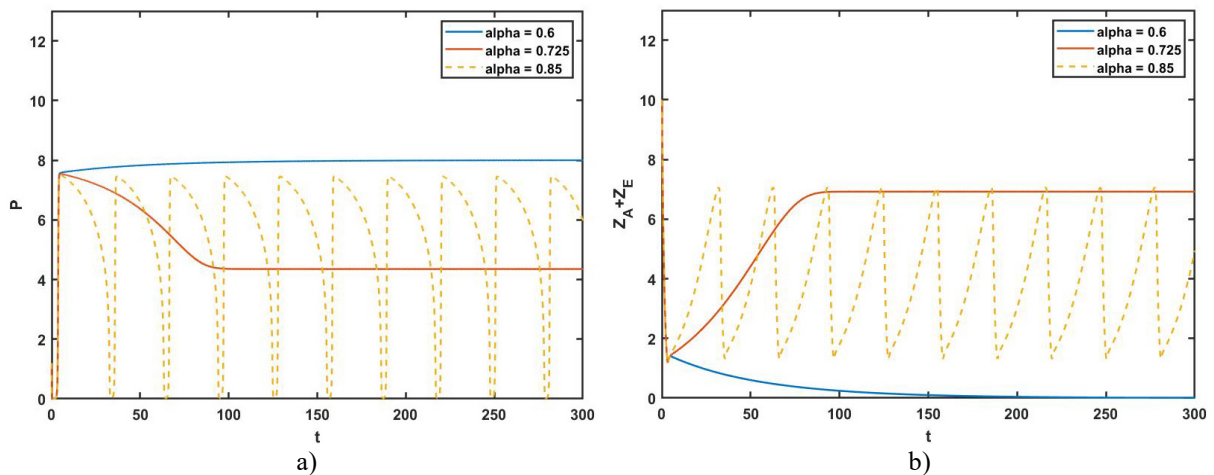


Fig. 5. The change of phytoplankton a) and zooplankton b) populations when modifying the value of transform rate.

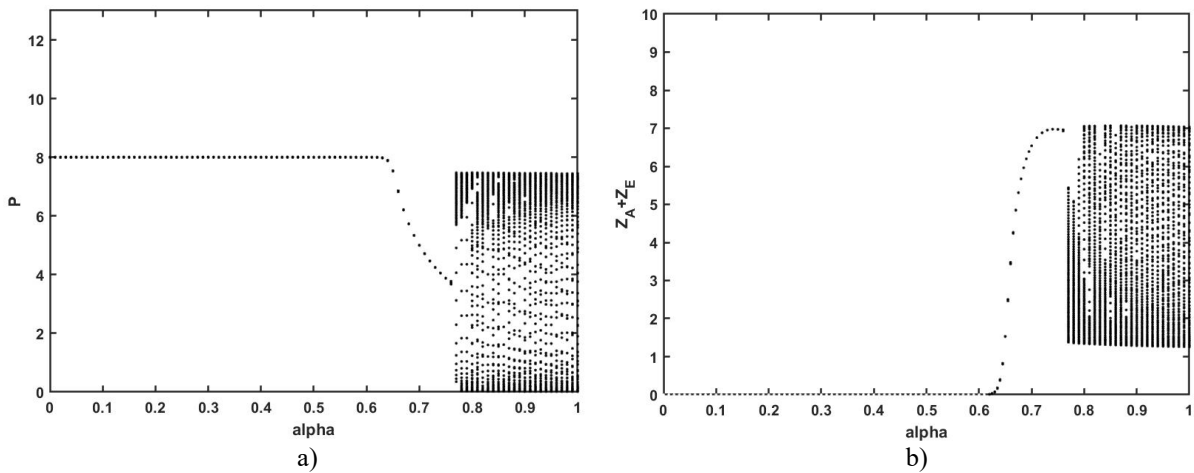


Fig. 6. Bifurcation diagrams respect to transform rate of phytoplankton a) and zooplankton b).

Fig. 5 shows the behavior of phytoplankton and total zooplankton density with three different values of transformation rate and keeping the other parameters unchanged. When the transformation rate is not great enough ($\alpha = 0.6$), the zooplankton population is extinct, and the phytoplankton population reaches the carrying capacity. When the transformation rate increases, the system can converge on the co-existence equilibrium point or limit cycle around this point. This phenomenon can be seen more clearly when observing the Hopf bifurcation diagram when varying the transformation rate in Fig. 6. When the transformation rate crosses a critical value, a limit cycle appears and breaks the stability at an equilibrium of the system. In conclusion, phytoplankton and zooplankton can co-exist only when the transformation parameters are great enough and the habitat has a suitable temperature.

5. Conclusion

In this paper, the interactions between zooplankton and phytoplankton under the temperature-affected and the stage structure in the zooplankton population were

studied. Our mathematical model was theoretically analyzed and illustrated by numerical simulation. The nonnegative and boundedness of solutions, existence, and uniqueness are indicated. With the given parameter value set, the best temperature range for co-existence in the system is about 12°C to 21°C . When the temperature is too low or high, the zooplankton is gradually eliminated, and the phytoplankton grows to the maximum capacity of the environment. On the other hand, for the parameter α , the system maintains the co-existence when its value is large enough. If this rate is too low, it leads to zooplankton being eliminated. About future work, in order to build a simulation model that is closer to natural phenomena, our current model can be improved by adding more complex factors such as the influence of light, nutrition, flow, etc.

Acknowledgments

This study is funded by Hanoi University of Science and Technology (HUST) under grant number T2022-PC-062. The authors would like to thank HUST for the financial support. We also thank the Anonymous reviewers for their careful reading of our manuscript and their many insightful comments and suggestions.

References

- [1] B. C. Rall, O. Vucic-pestic, R. B. Ehnes, M. Emmerson and U. Brose, Temperature, predator-prey interaction strength and population stability, *Global Change Biology*, 16, 2010, 2145-2157.
<https://doi.org/10.1111/j.1365-2486.2009.02124.x>
- [2] J. L. Lessard and D. B. Hayes, Effects of elevated water temperature on fish and macroinvertebrate communities below small dams, *River Research and Applications*, 19, 2003, 721-732.
<https://doi.org/10.1002/rra.713>
- [3] J. C. Morrill, R. C. Bales and M. H. Conklin, Estimating stream temperature from air temperature: implications for future water quality, *Journal of Environmental Engineering*, 131, 2005, 139-146.
[https://doi.org/10.1061/\(ASCE\)0733-9372\(2005\)131:1\(139\)](https://doi.org/10.1061/(ASCE)0733-9372(2005)131:1(139))
- [4] L. S. Peck, K. E. Webb and D. M. Bailey, Extreme sensitivity of biological function to temperature in antarctic marine species, *Functional Ecology*, 18, 2004, 625-630.
<https://doi.org/10.1111/j.0269-8463.2004.00903.x>
- [5] P. A. Staehr and K. A. J. Sand-Jensen, Seasonal changes in temperature and nutrient control of photosynthesis, respiration and growth of natural phytoplankton communities, *Freshwater Biology*, 51, 2, 2006, 249-262.
<https://doi.org/10.1111/j.1365-2427.2005.01490.x>
- [6] A. Toseland, S. J. Daines, J. R. Clark, A. Kirkham, J. Strauss, C. Uhlig, T. M. Lenton, K. Valentin, G. A. Pearson, V. Moulton and T. Mock, The impact of temperature on marine phytoplankton resource allocation and metabolism, *Nature Climate Change*, 3, 2013.
<https://doi.org/10.1038/nclimate1989>
- [7] K. E. Havens, R. M. Ointo-Coelho, M. Beklioglu, K. S. Christoffersen, E. Jeppesen, T. Lauridsen, A. Mazumder, G. Methot, B. P. Alloul, U. N. Tavsanoglu, S. Erdogan and J. Vijverberg, Temperature effects on body size of freshwater crustacean zooplankton from greenland to the tropics, *Hydrobiologia* 743, 2015, 27-35.
<https://doi.org/10.1007/s10750-014-2000-8>
- [8] J. G. Choi, T. C. Lippmann and E. L. Harvey, Analytical population dynamics underlying harmful algal blooms triggered by prey avoidance, *Ecological Modelling*, 481, 2023, 110366.
<https://doi.org/10.1016/j.ecolmodel.2023.110366>
- [9] A. Gera, R. Gayathri, P. Ezhilarasan, V. R. Rao and M.V.R Murthy, Coupled physical-biogeochemical simulations of upwelling, ecological response to fresh water, *Ecological Modelling*, 476, 2023, 110246.
<https://doi.org/10.1016/j.ecolmodel.2022.110246>
- [10] T. Chu, H. V. Moeller and K. M. Archibald, Competition between phytoplankton and mixotrophs leads to metabolic character displacement, *Ecological Modelling*, 481, 2023, 110331.
<https://doi.org/10.1016/j.ecolmodel.2023.110331>
- [11] A. Mandal, P. K. Tiwari and S. Pal, A nonautonomous model for the effects of refuge and additional food on the dynamics of phytoplankton-zooplankton system, *Ecological Complexity*, 46, 2021, 100927.
<https://doi.org/10.1016/j.ecocom.2021.100927>
- [12] K. Agnihotri and H. Kaur, Optimal control of harvesting effort in a phytoplankton-zooplankton model with infected zooplankton under the influence of toxicity, *Mathematics and Computers in Simulation*, 190, 2021, 946-964.
<https://doi.org/10.1016/j.matcom.2021.06.022>
- [13] S. N. Raw and S. R. Sahu, Strong stability with impact of maturation delay and diffusion on a toxin producing phytoplankton-zooplankton model, *Mathematics and Computers in Simulation*, 210, 2023, 547-570.
<https://doi.org/10.1016/j.matcom.2023.03.023>
- [14] Q. Zhao, S. Liu and X. Niu, Effect of water temperature on the dynamic behavior of phytoplankton - zooplankton model, *Applied Mathematics and Computation*, 378, 2020, 125211.
<https://doi.org/10.1016/j.amc.2020.125211>
- [15] J. M. Jackson and P. H. Lenz, Predator-prey interactions in the plankton: larval fish feeding on evasive copepods, *Sci Rep* 6, 33585, 2016.
<https://doi.org/10.1038/srep33585>
- [16] I. McLaren, Effects of temperature on growth of zooplankton, and the adaptive value of vertical migration, *Journal of the Fisheries Research Board of Canada*, 20, 2011, 685-727.
<https://doi.org/10.1139/f63-046>
- [17] W. Uszko, S. Diehl, G. Englund and P. Amarasekare, Effects of warming on predator-prey interactions - a resource-based approach and a theoretical synthesis, *Ecology Letters*, 20, 2017, 513-523.
<https://doi.org/10.1111/ele.12755>